Condensed Matter Theories
Volume 18

APPLICATION OF NON-LOCAL DENSITY FUNCTIONALS TO CLUSTERS, SURFACES AND VOIDS

Carlos Fiolhais

Department of Physics
and Center for Computational Physics, University of Coimbra
3004-516 Coimbra, Portugal

L. M. Almeida

Department of Physics, University of Aveiro
3810 Aveiro, Portugal
and Center for Computational Physics, University of Coimbra
3004-516 Coimbra, Portugal

1. INTRODUCTION

Various methods are available to solve the many-body quantum problem. Wavefunction methods, such as Hartree-Fock, Configuration Interaction and Quantum Monte-Carlo, aim at solving the Schrödinger equation obtaining, as accurately as possible wavefuntions and energy eigenvalues. A less computational demanding alternative is the Kohn-Sham self-consistent method [1] of Density Functional Theory [2], which allows to calculate the ground-state energy without knowing corresponding the many-body wavefunction, the only approximation lying in the exchange-correlation energy functional.

In the Local Spin Density Approximation (LSD) this exchange-correlation energy functional has the form

$$E_{xc}^{LSD}([n_\uparrow, n_\downarrow]) = \int d^3\mathbf{r}\; n(\mathbf{r}) f_{xc}^{LSD}(n_\uparrow(\mathbf{r}), n_\downarrow(\mathbf{r})), \tag{1}$$

where the electron density is $n = n_\downarrow + n_\uparrow$, with $n_\downarrow$ and $n_\uparrow$ respectively the up and down spin densities. By construction, the function E_{xc}^{LSD} is exact for the homogeneous electron gas. For a spin unpolarized system ($n_\uparrow = n_\downarrow = n/2$), the total density n is the only function to be considered in the Kohn-Sham equations. In that case LSD reduces to the Local Density Aproximation (LDA). One of the most used parametrizations in

the LSD (and the LDA) correlation is the Perdew-Wang formula (PW92) [3], which we adopt here.

For improving the exchange-correlation energy functional the Generalized Gradient Aproximation (GGA) has been developed. It includes explicitly density gradients besides the densities themselves:

$$E_{xc}^{GGA}([n_\uparrow, n_\downarrow]) = \int d^3\mathbf{r}\; n(\mathbf{r})\; f_{xc}^{GGA}(n_\uparrow(\mathbf{r}), n_\downarrow(\mathbf{r}), \nabla n_\uparrow, \nabla n_\downarrow). \tag{2}$$

This functional is semi-local, since it involves local density gradients. Perdew, Kurth and Ernzerhof constructed a GGA functional (PBE), which obeys simple physical constraints [4]. It became one of the most used in pratice. Other widely used GGA, which by contrast relies on the parametrization of an emprirical set of atomic data, is BLYP, due to Becke (exchange) [5] and Lee, Yang, and Parr (correlation) [6]. While the PBE is preferred by physicists, BLYP is more favoured by quantum chemists.

Recently, Perdew, Kurth, Zupan and Blaha [7] have proposed a generalization of GGA-PBE, the PKZB, which belongs to the more general class of Meta-GGA's. The form of a MGGA is

$$E_{xc}^{MGGA}([n_\uparrow, n_\downarrow]) = \int d^3\mathbf{r}\; n(\mathbf{r})\; f_{xc}^{MGGA}(n_\uparrow(\mathbf{r}), n_\downarrow(\mathbf{r}), \nabla n_\uparrow, \nabla n_\downarrow, \tau_\uparrow, \tau_\downarrow), \tag{3}$$

which has as input, besides the electronic densities and their gradients, the kinetic energy density

$$\tau_\sigma(\mathbf{r}) = \frac{1}{2} \sum_{\alpha}^{occup} |\nabla \psi_{\alpha\sigma}(\mathbf{r})|^2, \tag{4}$$

where $\psi_{\alpha\sigma}$ are the Kohn-Sham orbitals. MGGA is more non-local than GGA since it uses the orbitals, which are fully non-local functional of the densities. However, MGGAs are easy to implement in GGA codes, since the kinetic energy densities are available here.

Here we review our application of density functionals to jellium clusters and planar surfaces. Moreover, we present new results for the surface of real metals and for monoatomic voids.

2. JELLIUM MODEL CALCULATIONS

In the jellium model of metallic systems the ions are replaced by a continuous positive background. In spite of giving a qualitative unserstanding of the physics of simple metals, this model does not yield realistic results for the total energies of clusters, surfaces and solids. A remedy to this defect is the stabilized jellium model [8], in which the potential of the jellium model is replaced by a structureless pseudopotential such that the total energy is stable against density variation.

Nevertheless, the jellium model is useful as a benchmark of many-body theories. The quality of the above mentioned exchange-correlation approximations may be evaluated with the spherical jellium model. This admittedly simple model of metal

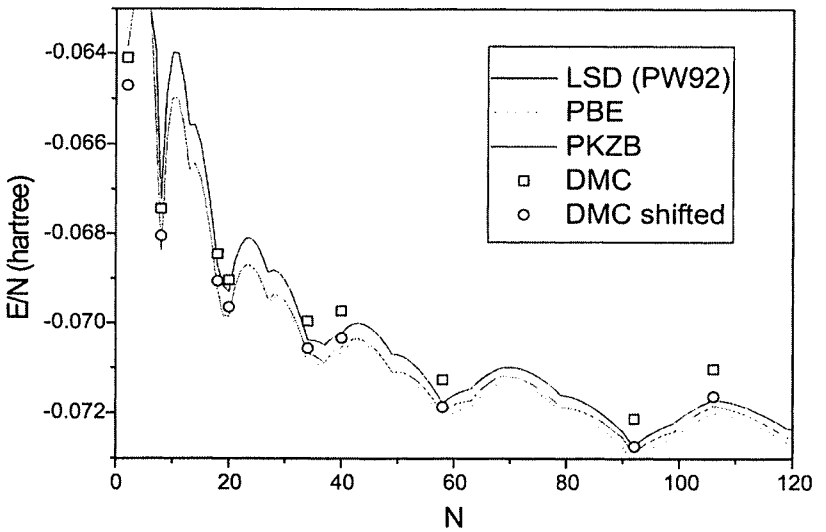

Figure 1. Total energies per electron (in hartree) for clusters with density parameter $r_s = 4.00$ bohr in different DFT approximations and in DMC. The DMC shifted points represent the DMC values (Ref. [10]) shifted by the fixed-node error found for the uniform electron gas.

clusters [9] is defined by just two parameters: the density parameter r_s and the total number of valence electrons N. Calculations using Quantum Monte Carlo methods are supposed to yield exact solutions to which the various DFT approximations should be compared. Recent Diffusion Monte Carlo (DMC) calculations made by Sottile and Ballone [10] are appropriate for this comparison.

We have solved the Kohn-Sham equations of DFT for a large range of jellium clusters and reported average deviations of total energies per electron for clusters of magic numbers with N=2, 8, 18, 20, 34, 40, 58, 92 and 106 electrons for densities r_s=1.00, 2.00, 3.25, 4.00 and 5.62 bohr [11]. The lowest average deviations were found for PKZB (0.0007 hartree) and PBE (0.0012 hartree) while LSD presents an average deviation of 0.0014 hartree. These results confirm that DFT is a very reliable method.

Actually, the calculations of Sottile and Ballone incorporate an error associated to the fixed-node approximation. We may estimate this error using the differences in parametrization of the correlation energy of the uniform electron gas made by Ortiz-Ballone [12] (which was fitted to fixed-node Quantum Monte Carlo results) and the LSD formula of Perdew-Wang 92 [3] (which was fitted to the released-node Quantum Monte Carlo results of Ceperley and Alder [13]). Although this estimation was made for the uniform electron gas (*i.e.*, for $N \to \infty$), we assume that it is valid for all cluster sizes. The effect of such correction on the Sottile and Ballone values is shown in Fig. 1.

The calculated average deviations of the various density functionals with respect to corrected DMC values is presented in Table 1, which is not much different from the corresponding table we have published before [11]. The conclusion is that the most correct DFT results for the energetics of jellium spheres are obtained from the

Table 1

Mean absolute deviations from released-node DMC (fixed-node values shifted by the estimated fixed-node error) of the total energies per electron (in hartree) of jellium clusters in various density functional approaches. The values are averages over nine magic clusters with N=2, 8, 18, 20, 34, 40, 58, 92, and 106 electrons.

r_s	LDA	BLYP	PBE	PKZB
1.00	0.0048	0.0110	0.0016	0.0023
2.00	0.0025	0.0117	0.0008	0.0011
3.25	0.0011	0.0110	0.0004	0.0003
4.00	0.0006	0.0105	0.0004	0.0003
5.62	0.0005	0.0093	0.0006	0.0006
average	0.0019	0.0107	0.0008	0.0009

PBE and PKZB exchange-correlation functionals.

Neglecting quantum oscillations due to the shell structure, the energy of a large neutral N-electron jellium sphere is given by the simple liquid drop model (LDM) formula [14]

$$E^{LDM} = \frac{4}{3}\pi R^3\alpha + 4\pi R^2\sigma + 2\pi R\gamma = \\ = \epsilon^{unif}N + 4\pi r_s^2\sigma N^{2/3} + 2\pi r_s\gamma N^{1/3}, \quad (5)$$

where α, σ and γ are parameters describing respectively the volume, surface and curvature energies, $R = r_s N^{-1/3}$ is the cluster radius, and $\epsilon^{unif} = (4\pi r_s^3/3)\alpha$ is the energy per electron of the uniform electron gas. The surface energy σ of jellium was calculated in Ref. [15] and the curvature energy γ in Ref. [16] both in the framework of LSD using only the self-consistent density profile of the planar surface. The energy per electron from Eq. (5) is then

$$\frac{E^{LDM}}{N} = \epsilon^{unif} + 4\pi r_s^2\sigma N^{-1/3} + 2\pi r_s\gamma N^{-2/3}. \quad (6)$$

From Fig. 2 we see that the LDM performs an average of the LSD energies as a function of $N^{-1/3}$. The same behaviour is observed with other density functionals. The oscillations around the LDM line of the different DFT approximations are about the same. Local minima are located at the shell-closing numbers N=2, 8, 20, 34, 40, 58, 92, and 106.

This fact leads to the following calculation of energy differences

$$\frac{E}{N} - \frac{E^{LSD}}{N} = (\epsilon^{unif} - \epsilon^{unif}_{PW92}) \\ + 4\pi r_s^2(\sigma - \sigma^{LSD})N^{-1/3} + 2\pi r_s(\gamma - \gamma^{LSD})N^{-2/3}. \quad (7)$$

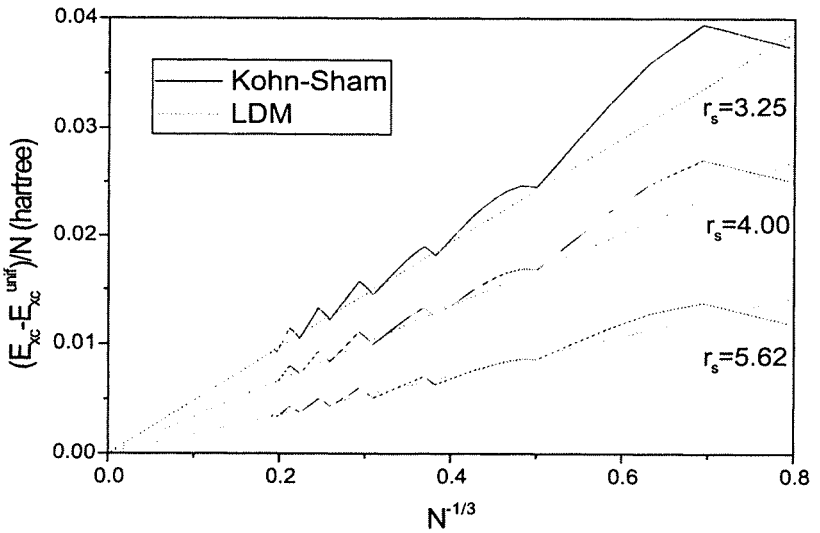

Figure 2. Deviation of the exchange-correlation energy per electron from its uniform electron gas value, $(E_{xc} - E_{xc}^{unif})/N$, using the Kohn-Sham equations in the LSD, for density parameters r_s=3.25, 4.00 and 5.62 bohr. For comparison we display the Liquid Drop Model (LDM), which includes the surface energy only: $E_{xc} = 4\pi r_s^2 \sigma_{xc} N^{-1/3}$.

Note that here E denotes a quantal energy and not the respective LDM approximation. Since the LSD surface energy $\sigma^{LSD}(r_s)$ is well-known [15,16] from planar surface calculations, we may extract the surface energy σ at any level of theory (including GGA, meta-GGA, and DMC) by evaluating the energies per electron within and beyond LSD and then fitting the difference as a function of $N^{-1/3}$ through Eq. (7), taking $\epsilon^{unif} - \epsilon_{PW92}^{unif}$, $\sigma - \sigma^{LDA}$ and $\gamma - \gamma^{LDA}$ as fit parameters. In Fig. 3 we see an example of this fitting procedure. The most striking feature is the disapearance of the significative oscillations around the LDM curves.

Table 2 shows the jellium exchange-correlation surface energies, calculated by two separated methods [11]: fits to jellium spheres and computation of semi-infinite systems which are the limit $N \to \infty$ of the latter. The total surface energies may be obtained by adding the kinetic and Hartree surface energies, which are the same irrespective of the employed functional (they are shown in the last column of the table). The similarity between the values of surface energies obtained from fits and from the planar surface code indicates the accuracy of the fitting method for extracting surface energies.

The DMC surface energies estimated from the planar surface calculation of Acioli and Ceperley [17] are 3566, 711 and 372 erg/cm^2 for r_s= 2.00, 3.25 and 4.00 respectively. These are substantially lower than the values extracted from jellium spheres which are close to PKZB and LSD values. Calculations of surface energies based on the Random Phase Approximation (RPA+) [18, 19], which are reported to be the most accurate jellium surface energies available, also shows similar values. We believe therefore on the accuracy of the DMC surface energies we have extracted from jellium spheres.

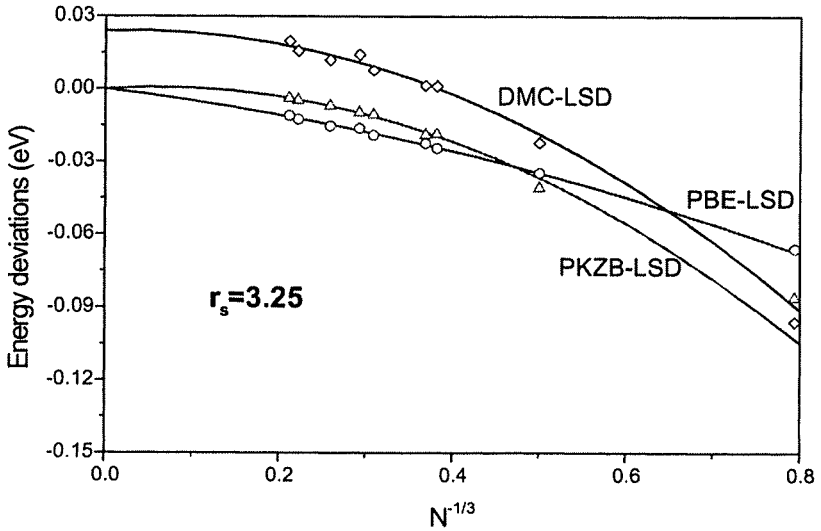

Figure 3. Energy deviations per particle from LSD of PBE (o), PKZB (Δ) and DMC($\diamond$) for jellium spheres with r_s=3.25 bohr, given by Eq. (7).

Table 2

Jellium exchange-correlation surface energies σ_{xc} (in erg/cm^2). Values calculated directly for a flat jellium surface are compared to those extracted from finite jellium spheres (fits). $\sigma_s + \sigma_h$ is the sum of kinetic and Hartree surface energies, so that the total surface energy is $\sigma = \sigma_s + \sigma_h + \sigma_{xc}$.

r_s	LSD	PBE fit	PBE	PKZB fit	PKZB	DMC fit	$\sigma_s + \sigma_h$
1.00	40928	40068	40276	41637	41463	41196	-109797
2.00	3357	3263	3263	3420	3400	3347	-4220
3.25	568.6	550.0	549.5	578.5	576.4	574.1	-347.7
4.00	261.7	252.6	252.5	265.9	265.6	272.8	-98.2
5.62	70.0	67.4	67.4	71.1	71.3	83.7	1.48

Although the curvature energy represents a small term of the total energy, its extraction from fitting is possible due to the good quality of the latter. In Table 3 we present the jellium curvature energies obtained by fitting (Ref. [11]) jellium clusters and LSD values interpolated from the results of Fiolhais and Perdew [16].

3. REAL METALS CALCULATIONS

In spite of the usefulness of the jellium model, realistic calculations of real metals

Table 3

Jellium curvature energies γ (in millihartree/bohr). The LSD values were interpolated using the formula $\gamma(r_s) = A\, {r_s}^{-B}\, exp(-r_s C)$, with A, B and C parameters fitted to γ values [16] at r_s = 2.07, 3.99, and 5.63 bohr (A=10.17271, B=1.580791, and C=0.289192).

r_s	LSD	BLYP	PBE	PKZB	DMC
1.00	7.62	5.84	6.13	3.26	1.77
2.00	1.91	1.15	1.58	0.87	0.76
3.25	0.62	0.33	0.53	0.27	0.27
4.00	0.36	0.19	0.31	0.15	0.10
5.62	0.13	0.07	0.11	0.04	-0.07

have to go beyond it. We have made calculations using the CRYSTAL98 [20], an all-electron DFT code which employs Gaussian basis sets. Some structural properties of simple metals (Be, Al, Mg, Li and Na) for various DFT exchange-correlation energy functionals have been reported elsewhere [21].

In order to calculate surface energies we have done a series of slab calculations [22]. Quantum size effects in slab energies are sizeable but there are several ways to extract surface energies from slab calculations [23]. The surface energies extracted from a series of slabs from 1 to 10 layers [22], adopting a method similar to that used in Ref. [23], are shown in Fig. 4.

As predicted by the jellium model, real metal MGGA-PKZB surface energies are close to LSD ones and higher than GGA-PBE ones. Moreover BLYP surface energies are strongly underestimated, in agreement again to the prediction of the jellium model. On the other hand, our LDA and GGA-PBE results are consistent with previous calculations [26] using Green's function Linear Muffin-Tin Orbitals in the atomic sphere aproximation.

Experimental data on surface energies are available but do not correspond to a direct measurement for the solid fase. They are obtained from the surface tension measurements in the liquid phase extrapolated to zero temperature. However these experimental data points also show that computation predictions are satisfactory (except for BLYP).

Still with the CRYSTAL98 code, we have done monovacancy calculations for the same five simple metals. We used the same basis set as in our previous metal bulk calculations [21]. The calculations were performed by the method of supercells for the unrelaxed monovacancy in the convencional crystal structures: bcc for Li and Na, fcc for Al and hcp for Be and Mg. In the case of bcc and fcc structures the monovacancies were calculated with 8, 27 and 64 atoms in the supercell in order to check the convergence with respect to supercell size. We have also verified the convergence with respect to the number of k-points. For the sake of simplicity, hcp

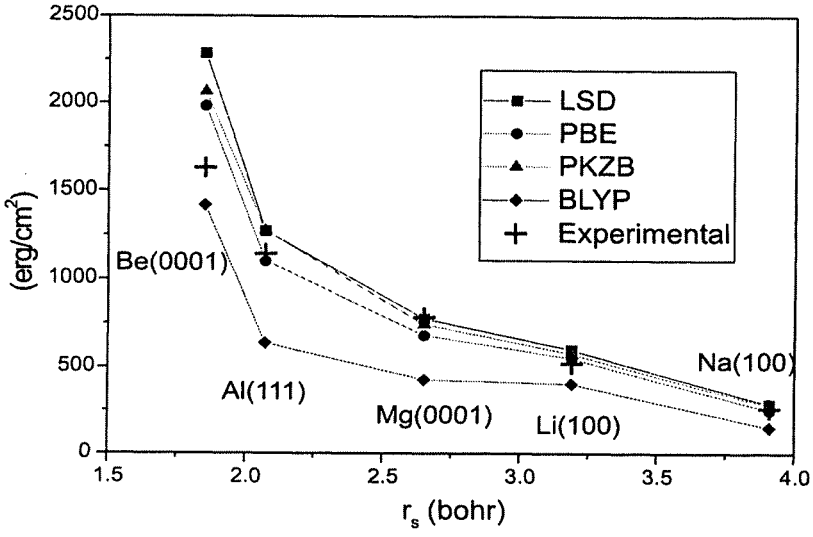

Figure 4. Total surface energies σ for real metals evaluated using CRYSTAL98. The exhibited valence electron densities correspond to the five simple metals Be, Al, Mg, Li and Na (r_s=1.85, 2.07, 2.65, 3.19 and 3.91, respectively). Experimental values are taken from Ref. [26].

calculations were only done in a supercell of 8 atoms.

The formation energy of the monovacancy E_{vac} is obtained by subtracting the total energy of the defect supercell with $N-1$ atoms by the corresponding $N-1$ atoms total energy of the supercell of the perfect bulk metal:

$$E_{vac} = E(N-1) - \frac{N-1}{N} E(N). \tag{8}$$

The calculated monovacancy formation energies are shown in Fig. 5.

Experimental values correspond obviously to a relaxed structure. The unrelaxed values should be higher than the experimental ones. However the atomic relaxation in monovacancies for simple metals might not lead to a significative reduction of formation energies. For aluminium, according to Mehl and Klein [24], the formation energy is only lowered by 0.05 to 0.03 eV when some atoms are allowed to relax about the vacancy.

4. CONCLUSIONS

Our calculations for the jellium model indicate that, accepting DMC as reference, MGGA-PKZB is a better functional for the jellium clusters and surfaces than the others. The LDM allows to extract surface energies from jellium clusters: both LSD and MGGA give accurate surface energies, in agreement with recent DMC results for clusters, but in disagreement with old DMC results for surfaces.

Considering real metals, we have verified that GGA-PBE and MGGA-PKZB yield in general a fair agreement with experimental data for bulk and surface systems.

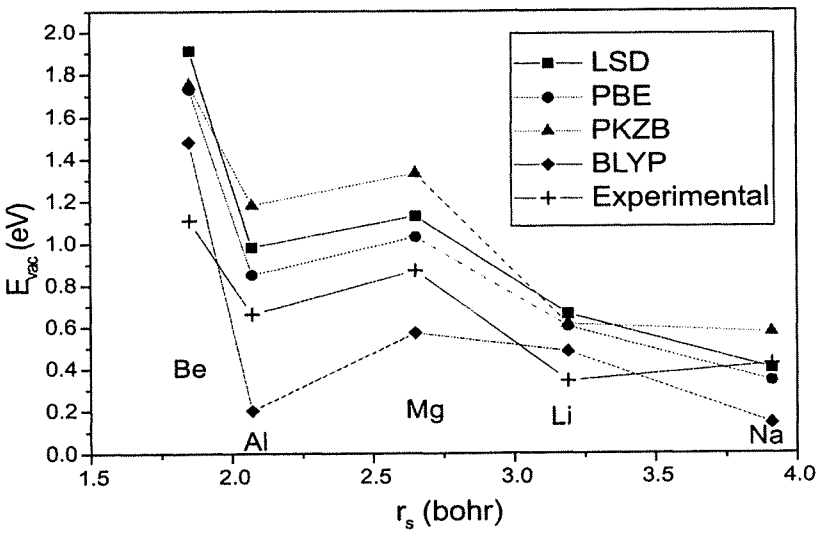

Figure 5. Unrelaxed monovacancy formation energies for some simple metals. Lattice constants used are the LDA ones found in Ref. [21] except for Al where we considered a =4.05 $\AA$ (the same value used in Ref. [24]). Experimental values are taken from Refs. [14] and [25].

On the contrary, chemical based GGA's like BLYP do not work well for these solids and surfaces. MGGA-PKZB seems to overestimate the vacancy formation energies. This is a puzzling result which should motivate further work.

ACKNOWLEDGMENT

We are grateful to Prof. John P. Perdew, from the Tulane University, New Orleans, USA, who collaborated in part of this work.

REFERENCES

[1] W. Kohn and L. J. Sham, *Phys. Rev.* **140**, A 1133 (1965).

[2] P. Hohenberg and W. Kohn, *Phys. Rev.* **136**, B864 (1964).

[3] J. P. Perdew and Y. Wang, *Phys. Rev. B* **45**, 13244 (1992).

[4] J. P. Perdew, K. Burke, and M. Ernzerhof, *Phys. Rev. Lett.* **77**, 3865 (1996).

[5] A. D. Becke, *Phys. Rev. A* **38**, 3098 (1988).

[6] C. Lee, W. Yang, and R. G. Parr, *Phys. Rev. B* **37**, 785 (1988).

[7] J. P. Perdew, S. Kurth, A. Zupan, and P. Blaha, *Phys. Rev. Lett.* **82**, 2544 (1999).

[8] J. P. Perdew, H. Q. Tran, and E. D. Smith, *Phys. Rev. B* **42**, 11627 (1990).

[9] M. Brack, *Rev. Mod. Phys.* **65**, 677 (1993).

[10] F. Sottile and P. Ballone, *Phys. Rev. B* **64**, 045105 (2001).

[11] L. M. Almeida, J. P. Perdew, and C. Fiolhais, *Phys. Rev. B* **66**, 075115 (2002).
[12] G. Ortiz and P. Ballone, *Phys. Rev. B* **50**, 1391 (1994).
[13] D. M. Ceperley and B. J. Alder, *Phys. Rev. Lett.* **45**, A 566 (1980).
[14] J. P. Perdew, Y. Wang, and E. Engel, *Phys. Rev. Lett.* **66**, 508 (1991).
[15] N. D. Lang and W. Kohn, *Phys. Rev. B* **1**, 4555 (1970).
[16] C. Fiolhais and J. P. Perdew, *Phys. Rev. B* **45**, 6207 (1992).
[17] P. H. Acioli and D. M. Ceperley, *Phys. Rev. B* **54**, 17199 (1996).
[18] Z. Yan, J. P. Perdew, S. Kurth, C. Fiolhais, and L. Almeida, Phys. Rev. B **61**, 2595 (2000).
[19] Z. Yan, J. P. Perdew, and S. Kurth, *Phys. Rev. B* **61**, 16430 (2000).
[20] V. R. Saunders, R. Dovesi, C. Roetti, M. Causà, N.M. Harrison, R. Orlando, and C.M. Zicovich-Wilson, *CRYSTAL98 User's Manual*, (University of Torino, Torino 1998).
[21] L. M. Almeida, C. Fiolhais, and M. Causà, *Int. J. Quant. Chem.*, to appear.
[22] L. M. Almeida and C. Fiolhais, *to be published.*
[23] V. Fiorentini and M. Methfessel, *J. Phys.: Condens. Matter* **8**, 6525 (1996).
[24] M. J. Mehl and B. M. Klein, *Physica B* **172**, 211 (1991).
[25] W. Hu, B. Zhang, B. Huang, F. Gao, and D. Bacon, *J. Phys: Condens. Matter* **13**, 1193 (2001).
[26] L. Vitos, A. V. Ruban, H. L. Skriver, and J. Kollár, *Surf. Sci.* **411**, 186 (1998).